Chao *et al. BMC Cancer* (2024) 24:1403
https://doi.org/10.1186/s12885-024-13125-5

BMC Cancer

RESEARCH

Open Access

Molecular profiling reveals novel therapeutic targets and clonal evolution in ovarian clear cell carcinoma

Angel Chao[1,2†], Chen-Yang Huang[3,4,5†], Willie Yu[4,5], Chiao-Yun Lin[1,2], Hao Lin[6], An-Shine Chao[1,7], Cheng-Tao Lin[1,2], Hung-Hsueh Chou[1,2], Kuang-Gen Huang[1,2], Huei-Jean Huang[1,2], Ting-Chang Chang[1,2], Steven G. Rozen[4,5,8], Ren-Chin Wu[2,9*] and Chyong-Huey Lai[1,2*]

Abstract

Background Ovarian clear cell carcinoma (OCCC) has a disproportionately high incidence among women in East Asia. Patients diagnosed with OCCC tend to experience worse clinical outcomes than those with high-grade serous carcinoma (HGSC) at advanced stages. The unfavorable prognosis of OCCC can be partly attributed to its frequent resistance to conventional chemotherapy. Within a precision medicine framework, we sought to provide a comprehensive molecular characterization of OCCC using whole-exome sequencing to uncover potential molecular targets that may inform novel therapeutic strategies.

Methods We performed whole-exome sequencing analysis on tumor-normal paired samples from 102 OCCC patients. This comprehensive genomic characterization of a substantial cohort of OCCC specimens was coupled with an analysis of clonal progression.

Results On analyzing 102 OCCC samples, *ARID1A* (67%) and *PIK3CA* (49%) emerged as the most frequently mutated driver genes. We identified tier 1 or 2 clinically actionable molecular targets in 40% of cases. This included DNA mismatch repair deficiency ($n=1$), as well as *BRCA2* ($n=1$), *PIK3CA* ($n=36$), $KRAS^{G12C}$ ($n=1$), and *ATM* ($n=4$) mutations. Furthermore, 45% of OCCC samples displayed *ARID1A* biallelic loss. Interestingly, we identified previously unreported mutations in the 5′ untranslated region of the *TERT* gene that harbored an adverse prognostic significance. Clock-like mutational processes and activated APOBECs were major drivers of somatic point mutations. Mutations arising from DNA mismatch repair deficiency were uncommon. Reconstruction of clonal evolution revealed that early genetic events likely driving tumorigenesis included mutations in the *ARID1A*, *PIK3CA*, *TERT*, *KRAS*, and *TP53* genes.

Conclusions Our study provides a comprehensive characterization of the genomic landscape and clonal evolution in OCCC within a substantial cohort. These findings unveil potentially actionable molecular alterations that could be leveraged to develop targeted therapies.

Keywords Ovarian clear cell carcinoma, Whole-exome sequencing, Clinical actionability, *TERT* mutation, Mutational signature, Clonal evolution

[†]Angel Chao and Chen-Yang Huang contributed equally to this work.

*Correspondence:
Ren-Chin Wu
qby@cgmh.org.tw
Chyong-Huey Lai
laich46@cgmh.org.tw
Full list of author information is available at the end of the article

Background

Ovarian cancer, primarily consisting of high-grade serous carcinoma (HGSC) and ovarian clear cell carcinoma (OCCC), is a major cause of cancer-related deaths in women, with an annual global death toll exceeding 200,000 [1, 2]. OCCC, which is notably associated with endometriosis, comprises 10 − 25% of ovarian cancers in East Asia compared to 5% in Western countries [3–5]. While OCCC is predominantly diagnosed at early stages (specifically I–II), HGSC is typically identified at advanced stages (namely III–IV). Accordingly, approximately two-thirds of OCCC cases are detected at an early stage, in contrast to only about one-fifth of HGSC cases [4]. Typically, OCCC has a more favorable prognosis than HGSC in the early stages [3–5]. However, as the disease progresses to advanced stages, the clinical outcomes for OCCC become less favorable compared to those of HGSC [6]. This is primarily attributed to the scarcity of targeted therapies and frequent chemoresistance [7].

Extensive research has characterized the somatic mutation landscape in HGSC [8, 9], demonstrating its prognostic value [10, 11]. Notably, mutations in genes such as *BRCA1, BRCA2*, *PALB2*, and *RAD51C* have been specifically associated with HGSC [12–15]. The molecular basis of OCCC, however, is less comprehensively understood. In contrast to HGSC, which is characterized by a high prevalence of *TP53* mutations, OCCC is distinguished by frequent mutations in the *ARID1A, PIK3CA*, *KRAS*, and *PPP2R1A* genes [16–20]. Nevertheless, most prior studies in this area have been limited by small sample sizes, leading to an incomplete understanding of the comprehensive genomic landscape of OCCC.

Within a precision medicine framework, this study aims to address this knowledge gap by investigating the mutation patterns in driver genes, somatic copy number alterations (SCNAs), mutational signatures, and clonal evolution of OCCC. Our research presents findings from a large cohort of 102 OCCC samples, for which whole-exome sequencing (WES) data were available. The current results have the potential to identify novel molecular targets that could inform the development of innovative treatment strategies.

Methods

Study participants, tissue specimens, and data collection

The Institutional Review Board of the Chang Gung Memorial Hospital (Taiwan) approved this study (IRB reference number: 202000143B0), which included a cohort of patients diagnosed with OCCC between 2016 and 2021. Tumor stages were determined using the *Federation Internationale de Gynecolgie et d'Obstetrique* (FIGO) guidelines [21]. Formalin-fixed, paraffin-embedded (FFPE) specimens were collected from the Linkou and Kaohsiung branches of the Chang Gung Memorial Hospital. Details of patient enrollment are illustrated in Fig. 1. OCCC is characterized by a combination of tubulocystic, papillary, and solid pattern with clear, eosinophilic, and hobnail cells [22]. In cases where peripheral blood samples were unavailable, normal samples were obtained from non-tumoral tissues, such as lymph nodes, fallopian tubes, or the uterus. Clinical and histopathological data, including age, stage, pathological features, and survival outcomes, were retrospectively collected from the patients' medical records.

DNA extraction and whole-exome sequencing

Genomic DNA was extracted from 10-μm FFPE sections of tumor and normal tissues using the QIAamp DNA FFPE Tissue Kit (Qiagen, Hilden, Germany), and from peripheral blood using the QIAamp DNA Blood Mini Kit (Qiagen). DNA concentration and integrity were assessed with the Quanti-iT dsDNA HS assay (Invitrogen, Carlsbad, CA, USA) and a fragment analyzer (Advanced Analytical Technologies, Ankeny, IA, USA), respectively. We used the Twist Human Core Exome EF Multiplex Complete Kit Enrichment (Twist Bioscience, South San Francisco, CA, USA) for library preparation. In brief, 50 ng of genomic DNA per sample was subjected to enzymatic fragmentation, and the resulting DNA fragments were subsequently used for library construction. Sequencing was performed on a Novaseq 6000 high-throughput sequencing platform (Illumina, San Diego, CA, USA).

Somatic single nucleotide variation and insertion-deletion calling

Exome reads were trimmed with trimmomatic (version 0.39) to remove adaptors and poor-quality sequences [23]. Subsequently, they were mapped to the human reference sequence GRCh38.p7 using BWA-mem (version 0.7.15) with default parameters [24]. Global mapping quality was evaluated using qualimap 2 (version 2.2.1) [25]. The median read depth for the tumor and normal tissue on the capturing target were 160 × (range: 95 − 255 ×) and 136 × (range: 74 − 452 ×), respectively (Supplementary Table S1).

Somatic single-base substitutions (SBSs) and small insertion and deletions (indels) were called using three different tools: MuTect2 (version 4.1.6.0), Strelka2 (version 2.9.2), and Varscan (version 2.3.9). Default parameters were used in all instances [26–28]. Somatic variants were selected based on the following criteria: (i) identification by at least two variant callers, (ii) a minimum read depth of 10 in normal samples and 20 in tumor samples, (iii) a mutated allele fraction of at least 0.1 for

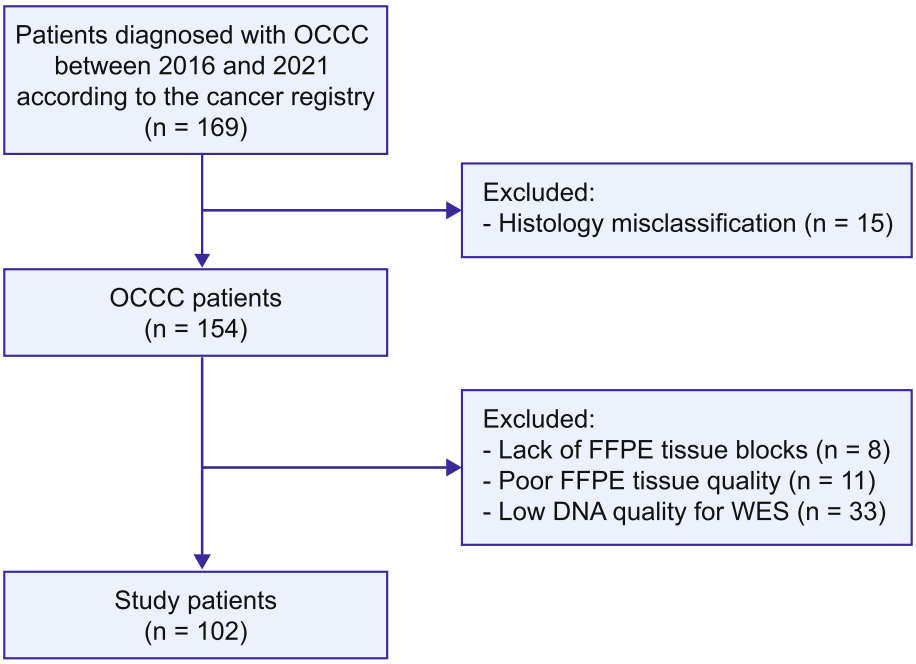

Fig. 1 Study flowchart. Patients diagnosed with ovarian clear cell carcinoma were retrospectively enrolled based on the registry data. The Systemized Nomenclature of Medicine (SNOMED) codes 87,000-A-M83103, 87,000-B-M83103, and 87,000-C-M83103 were used to identify the relevant cases. FFPE, formalin-fixed paraffin-embedded; WES, whole-exome sequencing

C > T and G > A variants (or 0.05 for others), and (iv) at least 7 supporting reads for C > T and G > A variants in the tumor sample (or 5 for others). SBSs and indels were annotated using wANNOVAR [29]. Gene driver status was determined using the COSMIC database [30]. Molecular targets were classified following the joint consensus of the Association for Molecular Pathology, American College of Medical Genetics and Genomics, American Society of Clinical Oncology, and College of American Pathologists [31].

Clinical actionability classification

The clinical actionability of the identified genetic alterations was categorized into two tiers. Tier 1 encompassed alterations with direct clinical implications and FDA-approved therapies specifically tailored for the given tumor type. Tier 2 included genetic alterations with FDA-approved treatments for different tumor types, as well as those linked to investigational therapies, and findings derived from meta-analyses, preclinical studies, and case reports.

Germline variant calling

We used freebayes (version 1.3.0) for calling germline variants and wANNOVAR for their annotation in normal samples [32]. Our analysis focused on 20 cancer-predisposing genes linked to an increased risk of ovarian cancer [33, 34], including *BRCA1, BRCA2, NTHL1, BRIP1, RAD51C, RAD51D, PALB2, ATM, MLH1, MLH3, MSH2, MSH3, MSH6, PMS1, PMS2, EPCAM, STK11, TP53,* and *CHEK2*. Germline variants were validated if they had an allele fraction over 0.2, read depth over 20, and were truncating mutations or known pathogenic variants listed in ClinVar [35].

Mutational signature assignment and spectrum reconstruction

Mutational signature assignment was conducted using the mSigAct R package (version 2.2) and the COSMIC database (version 3.2) [36, 37]. The *mSigAct::SparseAssignActivity* function was employed to quantify the contribution of SBS signatures in ovarian cancer mutational spectra [37]. Notably, SBS3, associated with homologous recombination deficiency, was only considered when more than five deletions with microhomology were present, whereas SBS6, SBS26, and SBS44, linked to DNA mismatch repair deficiency, were only applied when over 20 insertions in thymine homopolymer sequences were detected.

Somatic copy number alterations and genome doubling

Analysis of SCNAs was performed using the Sequenza software, version 3.0.0 [38], with default settings except for the parameter '–het 0.4' and a 200 kbp resolution.

The EstimateClonality R package was employed to infer the genome doubling (GD) status [39]. First, the average copy number (CN) at the chromosomal arm level was calculated from SCNA data. Subsequently, the *EstimateClonality::GD.function* was used to calculate a *p* value from 10,000 simulations, based on SCNA probabilities in each tumor, following previously established *p* value thresholds [39]. Tumors with *p* values below these cutoffs were classified as having undergone GD. The genomic instability index (GII) was defined as the fraction of the genome altered by somatic CN gains or losses, with a threshold of ≥ 1 compared to the background ploidy.

Consensus clustering on the somatic copy number alteration profile

The genome was partitioned into 5 MB bins by chromosome, and consensus clustering was performed using the *ConsensusClusterPlus* R package [40]. The clustering was based on the Euclidean distance with 10,000 iterations.

Timing of the clonal status

The clonal status of somatic mutations was assessed using a previously published method to determine the timing of their occurrence [41]. The analysis involved determining the fraction of cancer cells, estimating SCNAs, and evaluating the GD status. Specifically, the *MutationTimeR* package in R was applied, conducting 1,000 simulations to ascertain the timing of clonal events [41]. Detailed R scripts and the timing data for all somatic mutations are available at the GitHub repository (https://github.com/CYHuang-Lab/CGMH-OCCC-WES-project/).

Sanger sequencing of the *TERT* gene

The *TERT* gene promoter and 5' UTR were amplified using the KAPA HiFi HotStart PCR Kit (Roche, Basel, Switzerland) with two primer sets: promoter: 5'-GTC CTGCCCCTTCACCTT-3' (forward) and 5'-CAGCGC TGCCTGAAACTC-3' (reverse); 5' UTR: 5'-AGCCCC TCCCCTTCCTTT-3' (forward) and 5'-AGCACCTCG CGGTAGTGG-3' (reverse). The PCR cycling conditions included an initial denaturation at 95 °C for 3 min, followed by 35 cycles at 98 °C for 20 s, 60 °C for 15 s, and 72 °C for 15 s, with a final extension at 72 °C for 1 min. The PCR products were subsequently purified and subjected to Sanger sequencing.

Immunohistochemistry for WT1, napsin A, and HNF1B

Immunohistochemistry (IHC) was performed on a BOND-MAX automated stainer (Leica Biosystems, Nußloch, Germany) using the following primary antibodies and dilutions: WT1 (clone 6F-H2, Cell Marque, Rocklin, CA, USA; 1:100 dilution), napsin A (clone IP64, Leica Biosystems; 1:200 dilution), and HNF1B (catalog number 12533–1-AP, Proteintech, Rosemont, IL, USA; 1:100 dilution). Heat-induced epitope retrieval was carried out at 100 °C using a citrate-based pH 6.0 buffer (BOND Epitope Retrieval Solution 1, Leica Biosystems) for HNF1B and an EDTA-based pH 9.0 buffer (BOND Epitope Retrieval Solution 2, Leica Biosystems) for the remaining antibodies.

Statistical testing and survival analysis

All analyses were performed in R (version 4.1.0) with two-sided tests, unless specified otherwise. Categorical variables were compared with the Fisher's exact test, whereas the Wilcoxon rank-sum test was used to analyze continuous variables. Overall survival was measured from the date of pathological diagnosis of OCCC to the date of the last follow-up or death. The *survdiff* and *coxph* functions from the R survival package were employed. The *p* values were adjusted for multiple testing using the Benjamini–Hochberg method, which controls the false discovery rate. In this analysis, p values < 0.05 and q values < 0.1 were considered statistically significant.

Results

Patient characteristics

Supplementary Table S2 summarizes the clinical outcomes and genomic characteristics of the 102 patients included in the study. The median age of the participants was 52 years (range: 25 – 79 years). Most patients ($n = 72$, 70.6%) presented with stage I disease at diagnosis. The median follow-up duration was 28.9 months (range: 0.9–69.9 months).

Genomic landscape and driver mutations of OCCC

Figure 2 and Supplementary Fig. S1 depict the genomic profile of OCCC samples, revealing 5370 somatic SBSs and 580 indels impacting 4264 genes and the splicing junctions of 121 genes. The median non-silent mutations count was 46 (range: 3 – 521). Consistent with previous reports [16–20], *ARID1A* (66.7%) and *PIK3CA* (49%) were the most commonly mutated driver genes. Promoter or 5' UTR mutations of the *TERT* gene were identified in 26 (25.5%) tumors. Mutations were also frequently observed in *KRAS* (16.7%), *PPP2R1A* (15.7%), and *TP53* (6.9%). Enrichment analysis revealed that mutations in *ARID1A*, *PIK3CA*, *KRAS*, *PPP2R1A*, and *PIK3R1* were more prevalent in OCCC (Supplementary Fig. S2), whereas *TP53* has been reported to be frequently mutated in HGSC [8]. The *TP53*-mutated cases in our cohort were corroborated by immunohistochemical negativity for WT1, napsin A, and HNF1B. One patient (tumor OCCC-067) harbored a pathogenic germline mutation in *RAD51C* without a concurrent somatic *TP53*

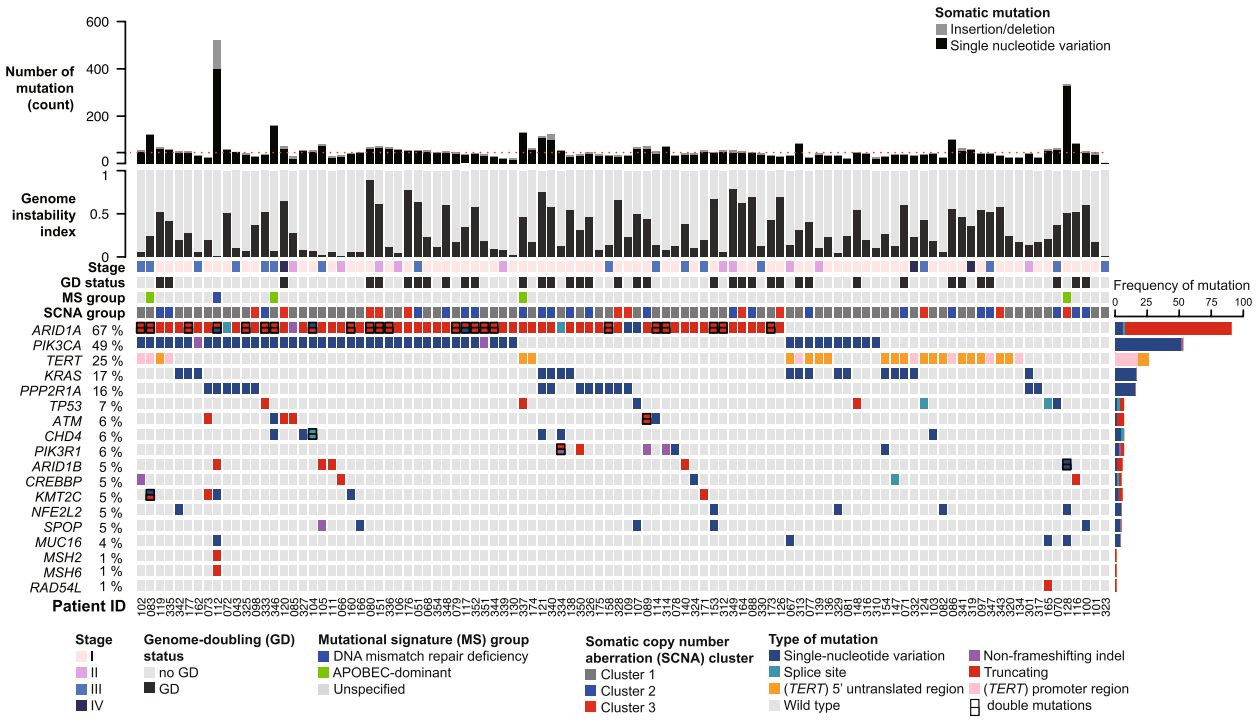

Fig. 2 Genomic landscape of 102 ovarian clear cell carcinoma samples. The rows represent the following data: counts of non-silent mutations, genome instability index, tumor stage, genome doubling (GD) status, mutational signature (MS) group, membership in somatic copy number alteration (SCNA) cluster, and non-silent somatic mutations in established cancer-driver genes (mutated in five or more tumors), as well as mutations in the TERT upstream region. Supplementary Fig. 1 illustrates mutations in known cancer-driver genes at lower frequencies

mutation (Supplementary Table S3). Additionally, a single tumor (OCCC-112) exhibited somatic mutations in both *MSH2* and *MSH6*, suggesting the rare occurrence of DNA mismatch repair deficiency in OCCC.

Mutational patterns and clinical actionability

The mutational patterns of *ARID1A, ATM,* and *TP53*, which were typical of tumor suppressor genes, were predominantly characterized by truncating mutations and an absence of hotspots (Fig. 3A, 3E, and 3F). Of the 91 non-silent *ARID1A* mutations, 91.2% (83 mutations) were truncating, 6.6% (6 mutations) were missense, and 2.2% (2 mutations) occurred at splice sites. In contrast, *PIK3CA*, *KRAS*, and *PPP2R1A* mutations were characterized by the presence of hotspots and an absence of truncating mutations (Fig. 3B, C, and D). *PIK3CA* exhibited hotspot mutations primarily at the H1047 ($n=17$), E542 ($n=9$), and E545 ($n=8$) positions (Fig. 3B), whereas the most common *KRAS* mutations were G12D ($n=7$) and G12V ($n=6$) (Fig. 3C). The prevalent *PPP2R1A* mutation identified in our cohort was R183W (11 out of 16) (Fig. 3D), a finding in line with previous research [42]. According to the current classification of clinical actionability in oncology [31], 41 out of 102 OCCC samples (40.2%) exhibited clinically actionable molecular targets. This encompassed tier 1 actionability in two specific tumors (2%): one exhibiting DNA mismatch repair deficiency (dMMR) and another with a somatic *BRCA2* mutation. Additionally, tier 2 actionability was identified in 39 tumors (37.5%), including 33 with *PIK3CA* mutations, three with *PIK3CA* and *ATM* mutations, one with a $KRAS^{G12C}$ mutation, one with a *RAD54L* mutation, and one with an *ATM* mutation.

A total of 91 non-silent mutations were identified in the *ARID1A* gene, with 83 being truncating mutations, potentially leading to a loss of function. Subsequently, we investigated the frequency of *ARID1A* deficiency due to biallelic loss using a previously described assessment method [43]. Biallelic loss was defined as the presence of either two truncating mutations, a single truncating mutation with loss of heterozygosity (LOH), or total copy number loss. The results revealed that 45.1% (46/102) of tumors exhibited biallelic loss of *ARID1A* (Fig. 3G), with 43.5% having two truncating mutations and 56.5% a single truncating mutation with LOH. Figure 4 summarizes the clinical actionability and the corresponding potential therapies for the study cohort.

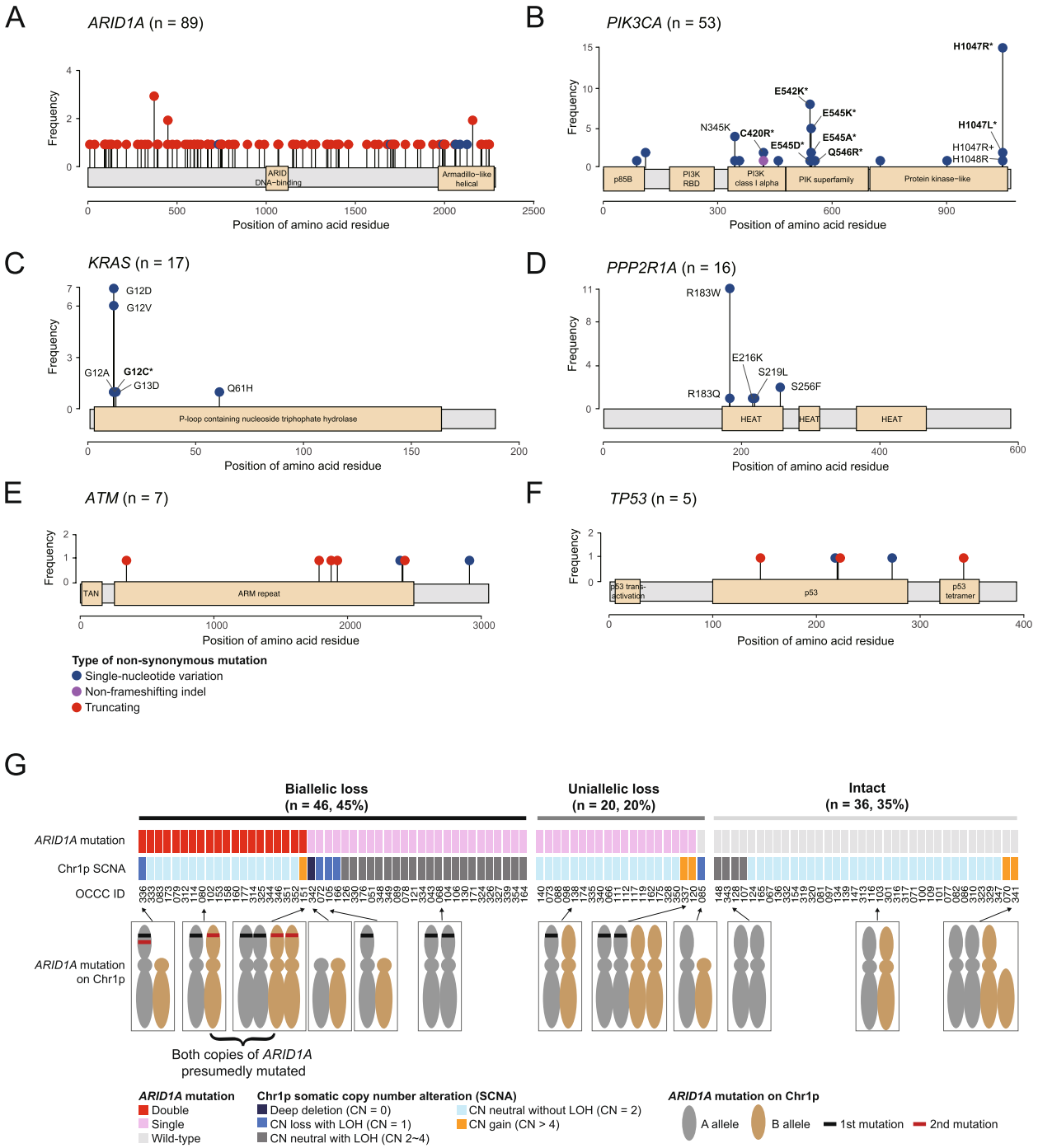

Fig. 3 Types and frequencies of mutations in six driver genes: (**A**) *ARID1A*, (**B**) *PIK3CA*, (**C**) *KRAS*, (**D**) *PPP2R1A*, (**E**) *ATM*, and (**F**) *TP53* gene. Selected mutation types were annotated accordingly. Mutations that fall within the tier 1 or 2 clinical actionability are emphasized using asterisk (*) markings. **G** Loss of tumor suppressor genes in the OCCC tumors. Biallelic loss is defined as having either of the following conditions: 1) double truncating mutations with or without loss-of-heterozygosity (LOH), 2) single truncating mutation with LOH, or 3) complete copy number loss (copy number of zero). Uniallelic loss is defined as having either of the following conditions: 1) single truncating mutation without LOH, 2) Copy number loss without truncating mutation

TERT mutations in the 5′ untranslated region correlated with poor outcomes

TERT mutations were identified in 25.5% (26/102) of OCCC samples (Fig. 5 and Supplementary Table S4), predominantly located in regulatory regions and notably creating novel ETS binding motifs. The majority of TERT mutations (18 of 26, 69%) were identified in the promoter region [44], whereas a significant proportion (8 of 26, 31%) was found in the less frequently studied 5′ UTR [45]. These mutations were collectively referred to as *TERT* upstream mutations. To ensure unbiased detection of *TERT* upstream mutations, we examined the sequencing coverage of the *TERT* upstream region (chr5:1,294,990–1,295,146) across our cohort. The median read depth was 99 (range: 26 – 235) for tumors and 60 (range: 21 – 299) for normal samples, with no significant difference between *TERT*-mutated and not mutated tumors (median: 99 *versus* 100, $p = 0.867$). Furthermore, Sanger sequencing validated 88.5% (23 out of 26) of these mutations, confirming the reliability of our findings (Supplementary Table S4). In our study, the most frequent *TERT* mutation was c.-124C > T (C228T), detected 15 times, followed by c.-57A > C (A161C) six times, c.-124C > A (C228A) twice, c.-54C > A (C158A) once, and c.-146C > T (C250T) once (Fig. 5A). We also discovered a novel complex indel (c.-29_-45 GTCCTGCTGCGCACGTG > A) in the 5′ UTR in one tumor. *TERT* promoter and 5′ UTR mutations were mutually exclusive. Consistent with a previous report [44], *TERT* mutations were more common in *ARID1A*-wild-type tumors (20 of 34, 58.8%) than in *ARID1A*-mutated tumors (6 of 68, 8.8%; two-sided Fisher's exact test, $p = 1.3 \times 10^{-7}$). Tumors with *TERT* 5′

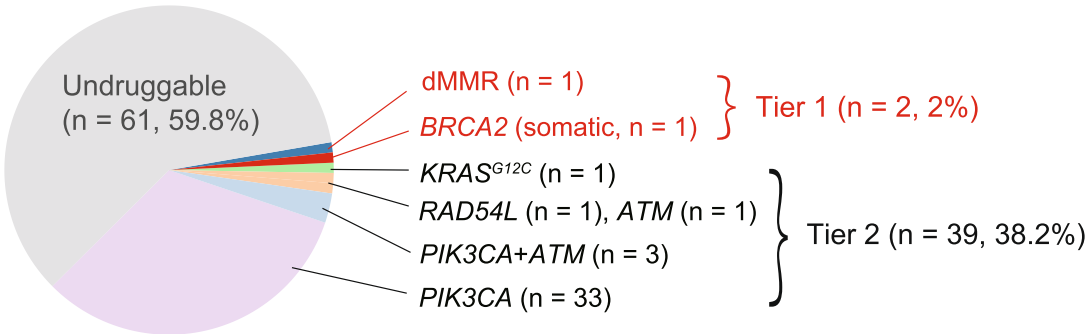

Tier	Molecular target	Alterations	Cancer types	Matched therapy	Number of tumor	(%)
I	MSI-H	NA	Ovarian cancer	Pembrolizumab	1	(1)
I	*BRCA2* (somatic)	N1766Kfs*2	Ovarian cancer	Olaparib, Rucaparib	1	(1)
II	*PIK3CA*	H1047R	Breast cancer	Alpelisib	15	(14.7)
II	*PIK3CA*	E542K	Breast cancer	Alpelisib	8	(7.8)
II	*PIK3CA*	E545K	Breast cancer	Alpelisib	5	(4.9)
II	*PIK3CA*	E545A	Breast cancer	Alpelisib	2	(2)
II	*PIK3CA*	H1047L	Breast cancer	Alpelisib	2	(2)
II	*PIK3CA*	C420R	Breast cancer	Alpelisib	2	(2)
II	*PIK3CA*	E545D	Breast cancer	Alpelisib	1	(1)
II	*PIK3CA*	Q546R	Breast cancer	Alpelisib	1	(1)
II	*KRAS*	G12C	Non-small cell lung cancer	Sotorasib, Adagrasib	1	(1)
II	*ATM*	Q2414X	Prostate cancer	Olaparib, Rucaparib	1	(1)
II	*ATM*	I346Nfs*2	Prostate cancer	Olaparib, Rucaparib	1	(1)
II	*ATM*	E1787X	Prostate cancer	Olaparib, Rucaparib	1	(1)
II	*ATM*	S1924X	Prostate cancer	Olaparib, Rucaparib	1	(1)
II	*ATM*	F1877Lfs*27	Prostate cancer	Olaparib, Rucaparib	1	(1)
II	*RAD54L*	F529Cfs*26	Prostate cancer	Olaparib, Rucaparib	1	(1)

Fig. 4 Clinical actionability of mutations identified in ovarian clear cell carcinoma specimens. Tier 1 alterations are those with direct clinical implications for a specific tumor type, including therapies approved by the FDA. Tier 2 includes alterations for which FDA-approved therapies exist for other tumor types, as well as investigational therapies, consensus findings from meta-analyses, preclinical studies, and case reports

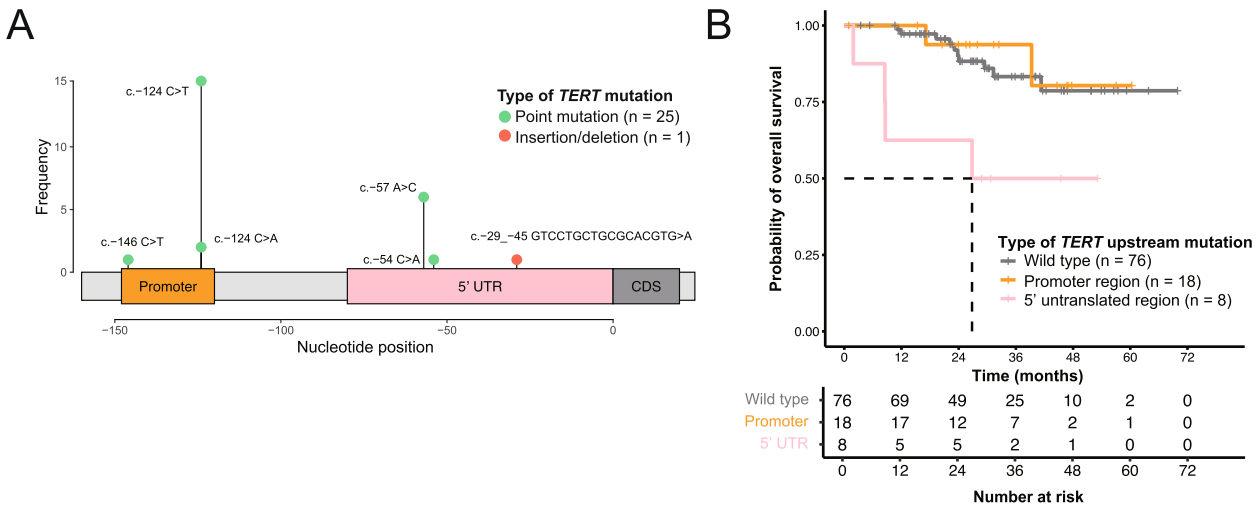

Fig. 5 *TERT* upstream mutations identified in ovarian clear cell carcinoma samples. **A** Classification and prevalence of *TERT* upstream mutations. **B** The presence 5′ UTR mutations was associated with significantly worse survival than lack of an upstream mutation or a mutation in the promoter region, as shown in both a univariate (HR = 4.49 *versus* wild type, $p = 0.011$) and a multivariable Cox proportional hazards analysis (HR = 3.86, *versus* wild type, $p = 0.025$, Supplementary Table S5). UTR, untranslated region; CDS, coding sequence

UTR mutations were associated with shorter overall survival (median, 26.8 months) compared to those without these mutations (median survival not reached, univariate hazard ratio [HR] = 4.49, 95% confidence interval [CI] = 1.4 to 14.34, $p = 0.011$, and multivariate HR = 3.86, 95% CI = 1.19 to 12.55, $p = 0.025$; Fig. 5B, Supplementary Tables S5 and 6). These findings suggest that *TERT* upstream mutations may serve as a prognostic marker in OCCC, warranting further validation in larger cohorts.

Mutational signature analysis

We identified a median of 143 SBSs (range: 21 to 1146) per tumor. Figure 6A and Supplementary Fig. S3 illustrate the distribution of SBS signatures across the examined OCCC samples. The clock-like signatures SBS1 and SBS5 were present in 94 (92.2%) and 86 (84.3%) of tumors, respectively, with a median of 25 (range: 0 to 308) and 89 (range: 0 to 291) mutations attributed to each. APOBEC-related signatures (SBS2 and SBS13) were identified in 42 (41.2%) of tumors. Notably, four malignancies (OCCC-083, 337, 346, and 128) exhibited high APOBEC mutational activity (median: 319 mutations, range: 238 to 844), without correlation to patient age, stage, driver mutations, or overall survival.

Somatic copy number alterations are pervasive and heterogeneous in OCCC

SCNAs are crucial for cancer progression and treatment response [46]. In our study, the median GII was 0.24, ranging from 0.01 to 0.89. A significant majority of OCCC samples (94.1%) showed copy number changes exceeding 1 in at least 5% of their genome. GD, a prevalent ploidy abnormality in cancer, was observed in 36.3% of samples. Although *TP53* mutations are linked to GD in other cancers [39], our findings in OCCC revealed no correlation between GD and driver mutations, including *TP53* variants (Supplementary Table S7). The most common SCNA in OCCC was 8q amplification, identified in over 60% of the tumors. Additional common amplifications were observed in 3q, 5p, and 17q, while copy-number losses were identified in 1p, 4q, 5q, 6q, 13q, 15q, and 17p (Fig. 6B). Approximately 20% of tumors exhibited copy-neutral LOH at 1p, affecting the *ARID1A* gene. SCNAs profiling divided OCCC tumors into three clusters (Supplementary Fig. S4): Cluster 1 (65.7%) with low-to-moderate instability and a low GD rate (13%); Cluster 2 (22.5%) with a high GD rate (95.7%) and extensive copy number loss; and Cluster 3 (11.8%) with a high GD rate, high genomic instability, and LOH. We observed a non-significant trend indicating potentially better survival outcomes for patients with tumors classified in SCNA Cluster 3 (Supplementary Fig. S5).

Timing of driver mutations during OCCC evolution

To investigate the timing of driver mutations in OCCC, we employed a previously described method [41, 47] that distinguishes mutations as clonal or subclonal based on variant allele fractions and SCNAs status (Fig. 7A). This approach further classifies clonal mutations as "early clonal", "late clonal", or "untimed clonal" depending on their copy number post-amplification

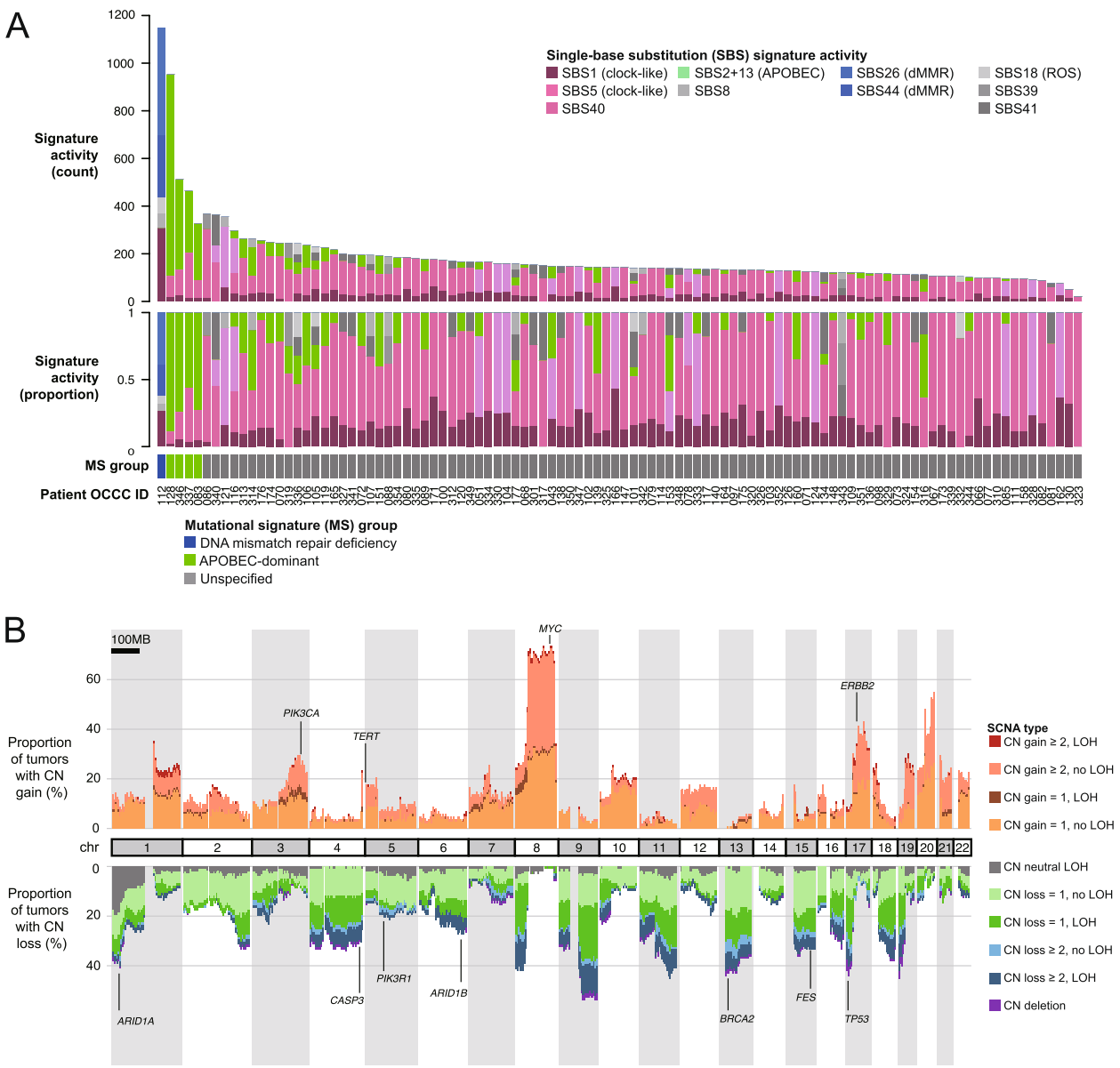

Fig. 6 **A** Single-base substitution (SBS) mutation signature activities across all 102 OCCCs. Mutation counts and the proportions of signatures contributing to the mutational spectrum of each tumor were shown in the top two panels. The bottom panel indicates tumors classified by the following "mutational signature groups": (1) DNA mismatch repair deficiency (OCCC-112), (2) APOBEC-dominant (OCCC-83, 128, 337, and 346). **B** Genome-wide somatic copy number alteration (SCNA) patterns observed in the OCCC cohort

(Fig. 7A). There were 3,098 early clonal mutations, 1,822 late clonal mutations, 8,120 untimed clonal mutations, and 6,628 subclonal mutations. Genes with a high frequency of early clonal and untimed clonal mutations – such as *ARID1A*, *PIK3CA*, *TERT*, and *KRAS* – are implicated in tumor initiation (Fig. 7B). Notably, *ARID1A*, *TERT*, and *PIK3CA* mutations were predominantly clonal compared to non-driver genes (Supplementary Table S8, two-sided Fisher's exact test with a Benjamini–Hochberg correction, q values of 1.044×10^{-6}, 0.0015, and 0.0746, respectively).

Discussion

OCCC is notably resistant to conventional chemotherapy, particularly regimens based on platinum and taxanes, which are standard first-line treatments for ovarian cancer [3–5]. This chemoresistance is attributed to several key factors, including the inherently low proliferation rate of OCCC, which limits the efficacy

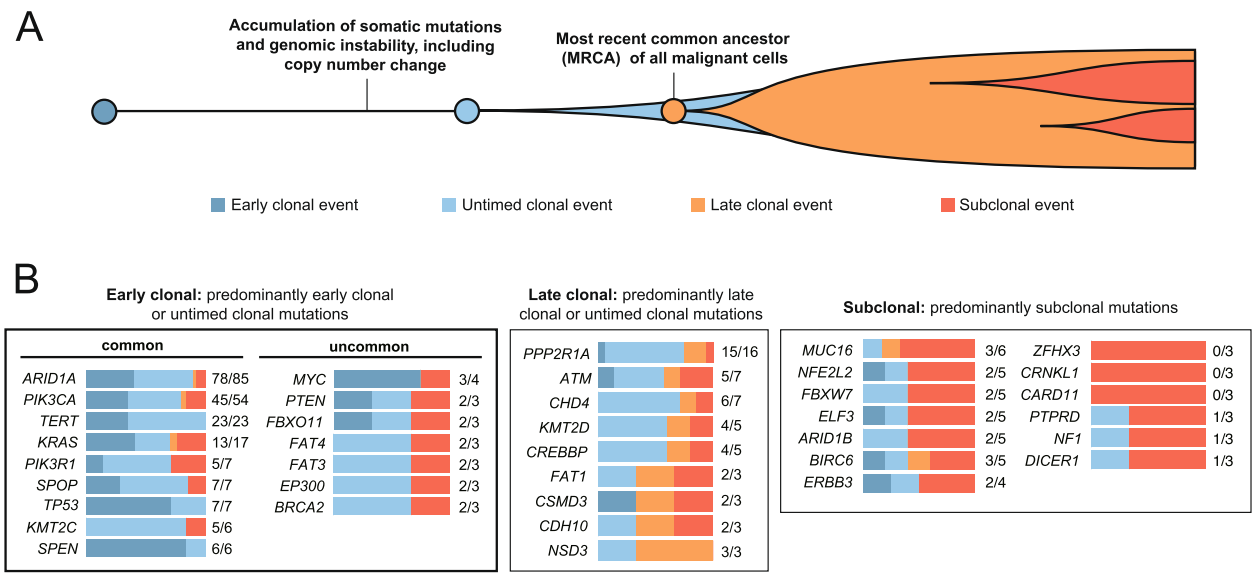

Fig. 7 Driver mutation timing estimates in ovarian clear cell carcinoma specimens. **A** Based on the timing of somatic mutations relative to somatic copy number change at the same locus, we categorized clonal mutation events as "early clonal" (occurring before the copy-number gain), "untimed clonal" (inability to determine the timing relative to the somatic copy-number gain), and "late clonal" (occurring after the somatic-copy-number gain). **B** Driver genes were grouped according to the timing and clonality of the identified somatic mutations. Color bars to the right of each gene symbol indicate the proportions of early clonal (dark blue), untimed clonal (light blue), late clonal (orange), and subclonal (dark orange) mutations for each gene. The values displayed to the right of the bar graph indicate the number of clonal mutations and the total mutation count within each specified gene. Genes categorized as "early clonal" are identified as potential key factors in the initiation of OCCC

of chemotherapeutic agents. Moreover, OCCC cells frequently display reduced drug accumulation and enhanced drug detoxification mechanisms, which further compromise the clinical efficacy of chemotherapy. Notwithstanding extensive research endeavors, a tailored chemotherapy regimen specifically designed for OCCC remains elusive. Consequently, elucidating the molecular underpinnings of this malignancy is crucial for identifying novel therapeutic targets and developing more effective treatment strategies. Our comprehensive study of OCCC genomic profile revealed that only 2% (2 out of 102) of samples had tier 1 clinically actionable targets, which are suitable for routine clinical use. These included one case with dMMR and another with a *BRCA2* mutation. Notably, *BRCA2* mutations can respond favorably to poly ADP-ribose polymerase inhibitors, which have been approved for advanced ovarian cancer [48, 49]. Similarly, an immune checkpoint inhibitor targeting the PD-1 pathway is available for advanced dMMR malignancies [50]. Tier 2 clinical actionability – which refers to investigational molecular targets – was more common, being identified in 38.2% (39/102) of the analyzed samples. This category included mutations in the *PIK3CA*, *KRAS*, *RAD54L*, and *ATM* genes. *PIK3CA* mutations are of particular interest due to their potential responsiveness to alpelisib, a selective inhibitor of the PI3Kα protein. This drug is currently approved for *PIK3CA*-mutated breast cancer [51], and its efficacy in treating ovarian cancer is currently under investigation [52]. *ERBB2* amplification has also emerged as a promising therapeutic target in OCCC [53]. To expand the feasibility and applicability of targeted therapy clinical trials for OCCC, it is recommended to include *ERBB2* amplification as a criterion for patient enrollment in basket trials designed to target this specific genetic alteration. Similarly, covalent inhibitors like sotorasib and adagrasib have shown promise in treating non-small-cell lung cancer harboring the $KRAS^{G12C}$ mutation [54, 55]. Moreover, inhibitors targeting the $KRAS^{G12D}$ mutation have demonstrated encouraging clinical responses [56].

In addition to tier 1 and 2 actionable mutations, our analysis revealed that biallelic loss of *ARID1A* [57] was present in 45% of the examined samples. This observation implies that the preclinical investigation of EZH2 inhibitors, which have shown promise in suppressing the growth of *ARID1A*-mutated cancers [58], may be a viable avenue for further exploration. Additionally, mutations in *PPP2R1A* were detected in 16% of the samples, potentially affecting cell growth through alterations in the Aα subunit of serine/threonine phosphatase 2A (PP2A) [42]. These mutations may be amenable to targeting with ribonucleotide reductase inhibitors [59].

Our analysis also confirmed the involvement of the *TERT* gene in the pathogenesis of OCCC [44]. with

mutations in the *TERT* promoter and 5' UTR being identified in 17.6% and 7.8% of samples, respectively. This is, to our knowledge, the first study to report the occurrence of *TERT* 5' UTR mutations in OCCC. These mutations could lead to increased TERT expression and telomerase activation. Mutations in the *TERT* promoter create a de novo binding motif for transcription factors, whereas mutations in the 5' UTR disrupt the connection between the repressor complex MAX/Mad1 and the E-box sequence (CACGTG) [60]. Notably, OCCC patients with *TERT* 5' UTR mutations exhibited poorer survival outcomes compared to those with *TERT* promoter mutations or no mutations, suggesting the clinical relevance of this molecular pathway. While directly targeting *TERT* or its promoter mutations is challenging due to the complex role of telomerase in cancer [45], these variants may influence responses to certain therapies, such as BRAF and MEK inhibitors [60]. This highlights the potential of *TERT* mutations in guiding the development of targeted treatments for OCCC.

Our study not only identified molecular changes that could serve as a foundation for preclinical exploration of novel therapeutic strategies, but also provided evidence supporting the hypothesis that OCCC originates from endometriotic cells, in line with the "precursor escape" model [61]. This framework proposes that endometriotic cells gradually amass genetic alterations, eventually giving rise to OCCC. Our analysis of OCCC samples also revealed early clonal mutations in the *KRAS* and *PIK3CA* genes. Similar variants have been previously reported in endometriotic epithelium [62], suggesting these genetic alterations may be involved in OCCC initiation.

The molecular context of the 5' UTR *TERT* mutations identified in our study can be inferred from the findings of Huang et al. [45]. They reported that the c.-57A > C (A161C) mutation generates a "(T/A)TCC" sequence, which is a de novo putative ETS-transcription factor binding motif. Similarly, the c.-54C > A (C158A) mutation creates a CCGGAA/T motif, which is a potential binding site for ETS transcription factors. These mutations were found to correlate with upregulated *TERT* mRNA expression and increased telomerase activity in adult gliomas. Furthermore, we identified a novel complex indel (c.-29_-45 GTCCTGCTGCGCACGTG > A) in the 5' UTR of *TERT*, which contains canonical E-box (CACGTG) elements. Previous research has shown that this E-box element mediates repression of *TERT* transcription in a renal cell carcinoma cell line derivative (RCC23 + 3) with a transferred copy of normal human chromosome 3 [63]. Taken together, these findings suggest that the 5' UTR *TERT* mutations may enhance the transcriptional activity of the *TERT* core promoter.

Regarding frequently altered genes and their prognostic implications in OCCC, our study identified an association between 5' UTR *TERT* mutations and reduced overall survival. While mutations upstream of the *TERT* promoter are recognized as significant prognostic markers in OCCC [44], it is important to note that the median follow-up period for our cohort was relatively short (2.5 years) and the occurrence of these genetic alterations was limited. Notably, other genetic mutations, such as those in *ARID1A* and *PIK3CA*, have been associated with unfavorable prognosis in a smaller series of 55 patients [64]. In a separate study, the loss of ARID1A expression was identified as a negative prognostic factor in 9 out of 60 patients with OCCC who received platinum-based chemotherapy [65]. However, these findings are preliminary and should be interpreted with caution. To derive more reliable conclusions, further validation is essential, particularly in larger cohorts with extended follow-up periods. Moreover, comprehensive molecular investigations are necessary to fully elucidate the role of frequently altered genes in OCCC.

In the current study, we found that SCNA was prevalent and heterogeneous in OCCC. In particular, we identified a group of OCCCs with high degree of genomic instability and better survival outcomes in this SCNA cluster 3 group. Previously, *TP53* mutation and homologous recombination deficiency may contribute to the genomic instability and genome doubling [39, 66]. However, the exact molecular mechanisms underlies the genomic instability is not fully characterized. Our study demonstrated that extent of SCNA in OCCC may represent a potential prognostic marker, necessitating validation in a larger cohort.

In conclusion, the current study offers a thorough analysis of the genomic alterations and clonal progression in OCCC, uncovering numerous mutations that could be targeted by novel pharmacological treatments. The study also supports the hypothesis that OCCC originates from endometriotic epithelium. These insights have the potential to form the foundation for advancements in precision oncology, facilitating the development of more effective therapeutic strategies for patients with OCCC.

Abbreviations

CI	Confidence interval
CN	Copy number
dMMR	Mismatch repair deficiency
FFPE	Formalin-fixed, paraffin-embedded
GD	Genome doubling
GII	Genomic instability index
HGSC	High-grade serous carcinoma
HR	Hazard ratio
LOH	Loss of heterozygosity
MS	Mutational signature
IRB	Institutional review board
OCCC	Ovarian clear cell carcinoma
PP2A	Phosphatase 2A

SCNAs	Somatic copy number alterations
SBSs	Somatic single-base substitutions
UTR	Untranslated region
WES	Whole-exome sequencing

Supplementary Information

The online version contains supplementary material available at https://doi.org/10.1186/s12885-024-13125-5.

Supplementary Material 1.

Acknowledgements
This study was financially supported by a grant (CIRPG 3K0031/2) from the Chang Gung Medical Foundation.

Authors' contributions
AC, RCW, and CHL designed the study. AC, CYL, and RCW performed the experiments. AC, CYH, SGR, and RCW analyzed and interpreted the data. RCW performed the pathology assessment and Sanger sequencing. AC, CHL, ASC, CTL, HHC, KGH, HJH, TCC, and CHL collected patient samples and clinical data. WY performed the sequencing data encryption and uploaded to EGA. AC and CYH wrote the manuscript. SGR, RCW, and CHL reviewed and edited the manuscript. The final manuscript was read and approved by all authors.

Data availability
The catalog of somatic mutations, SCNA estimations, and mutation timing analyses from the study cohort are accessible at the following GitHub repository: https://github.com/CYHuang-Lab/CGMH-OCCC-WES-project/. Tumor and normal exome sequencing data have been deposited at the European Genome-phenome Archive (EGA, http://www.ebi.ac.uk/ega/; accession number EGAS50000000031). The R codes utilized in this study are accessible at https://github.com/CYHuang-Lab/CGMH-OCCC-WES-project/.

Declarations

Ethics approval and consent to participate
This study was approved by the Institutional Review Board of the Chang Gung Memorial Hospital (reference number: 202000143B0). Given the retrospective nature of the analysis, the requirement for informed consent was waived.

Consent for publication
All authors have provided their consent for the publication of this manuscript.

Competing interests
The authors declare no competing interests.

Author details
[1]Department of Obstetrics and Gynecology, Linkou Chang Gung Memorial Hospital and Chang Gung University, College of Medicine, 5, Fuxing St., Guishan Dist., Taoyuan City 333, Taiwan. [2]Gynecologic Cancer Research Center, Linkou Chang Gung Memorial Hospital and Chang Gung University, College of Medicine, Taoyuan City 333, Taiwan. [3]Division of Hematology-Oncology, Department of Internal Medicine, Linkou Chang Gung Memorial Hospital and Chang Gung University, College of Medicine, Taoyuan City 333, Taiwan. [4]Center for Computational Biology, Duke-NUS Medical School, Singapore 169857, Singapore. [5]Programme in Cancer and Stem Cell Biology, Duke-NUS Medical School, Singapore 169857, Singapore. [6]Department of Obstetrics and Gynecology, Kaohsiung Chang Gung Memorial Hospital, Kaohsiung City 833, Taiwan. [7]Department of Obstetrics and Gynecology, New Taipei City Municipal Tucheng Hospital, New Taipei City 236, Taiwan. [8]Cancer Therapeutics Research Laboratory, Division of Medical Sciences, National Cancer Center Singapore, Singapore 169610, Singapore. [9]Department of Pathology, Linkou Chang Gung Memorial Hospital and Chang Gung University College of Medicine, 5, Fuxing St., Guishan Dist., Taoyuan City 333, Taiwan.

Received: 12 September 2024 Accepted: 29 October 2024
Published online: 14 November 2024

References

1. Cabasag CJ, Fagan PJ, Ferlay J, Vignat J, Laversanne M, Liu L, van der Aa MA, Bray F, Soerjomataram I. Ovarian cancer today and tomorrow: A global assessment by world region and Human Development Index using GLOBOCAN 2020. Int J Cancer. 2022;151(9):1535–41.
2. Sung H, Ferlay J, Siegel RL, Laversanne M, Soerjomataram I, Jemal A, Bray F. Global Cancer Statistics 2020: GLOBOCAN Estimates of Incidence and Mortality Worldwide for 36 Cancers in 185 Countries. CA Cancer J Clin. 2021;71(3):209–49.
3. Ku FC, Wu RC, Yang LY, Tang YH, Chang WY, Yang JE, Wang CC, Jung SM, Lin CT, Chang TC, et al. Clear cell carcinomas of the ovary have poorer outcomes compared with serous carcinomas: Results from a single-center Taiwanese study. J Formos Med Assoc. 2018;117(2):117–25.
4. Chan JK, Teoh D, Hu JM, Shin JY, Osann K, Kapp DS. Do clear cell ovarian carcinomas have poorer prognosis compared to other epithelial cell types? A study of 1411 clear cell ovarian cancers. Gynecol Oncol. 2008;109(3):370–6.
5. del Carmen MG, Birrer M, Schorge JO. Clear cell carcinoma of the ovary: a review of the literature. Gynecol Oncol. 2012;126(3):481–90.
6. Peres LC, Cushing-Haugen KL, Kobel M, Harris HR, Berchuck A, Rossing MA, Schildkraut JM, Doherty JA. Invasive Epithelial Ovarian Cancer Survival by Histotype and Disease Stage. J Natl Cancer Inst. 2019;111(1):60–8.
7. Huang HJ, Yang LY, Tung HJ, Ku FC, Wu RC, Tang YH, Chang WY, Jung SM, Wang CC, Lin CT, et al. Management and clinical outcomes of patients with recurrent/progressive ovarian clear cell carcinoma. J Formos Med Assoc. 2020;119(4):793–804.
8. The Cancer Genome Atlas Research Network. Integrated genomic analyses of ovarian carcinoma. Nature. 2011;474(7353):609–15.
9. Cheng Z, Mirza H, Ennis DP, Smith P, Morrill Gavarro L, Sokota C, Giannone G, Goranova T, Bradley T, Piskorz A, et al. The Genomic Landscape of Early-Stage Ovarian High-Grade Serous Carcinoma. Clin Cancer Res. 2022;28(13):2911–22.
10. Garsed DW, Pandey A, Fereday S, Kennedy CJ, Takahashi K, Alsop K, Hamilton PT, Hendley J, Chiew YE, Traficante N, et al. The genomic and immune landscape of long-term survivors of high-grade serous ovarian cancer. Nat Genet. 2022;54(12):1853–64.
11. Yang SYC, Lheureux S, Karakasis K, Burnier JV, Bruce JP, Clouthier DL, Danesh A, Quevedo R, Dowar M, Hanna Y, et al. Landscape of genomic alterations in high-grade serous ovarian cancer from exceptional long- and short-term survivors. Genome Med. 2018;10(1):81.
12. Harter P, Hauke J, Heitz F, Reuss A, Kommoss S, Marme F, Heimbach A, Prieske K, Richters L, Burges A, et al. Prevalence of deleterious germline variants in risk genes including BRCA1/2 in consecutive ovarian cancer patients (AGO-TR-1). PLoS ONE. 2017;12(10):e0186043.
13. Risch HA, McLaughlin JR, Cole DE, Rosen B, Bradley L, Kwan E, Jack E, Vesprini DJ, Kuperstein G, Abrahamson JL, et al. Prevalence and penetrance of germline BRCA1 and BRCA2 mutations in a population series of 649 women with ovarian cancer. Am J Hum Genet. 2001;68(3):700–10.
14. Arcieri M, Andreetta C, Tius V, Zapelloni G, Titone F, Restaino S, Vizzielli G. Molecular biology as a driver in therapeutic choices for ovarian cancer. Int J Gynecol Cancer. 2024.
15. Pietragalla A, Arcieri M, Marchetti C, Scambia G, Fagotti A. Ovarian cancer predisposition beyond BRCA1 and BRCA2 genes. Int J Gynecol Cancer. 2020;30(11):1803–10.
16. Shibuya Y, Tokunaga H, Saito S, Shimokawa K, Katsuoka F, Bin L, Kojima K, Nagasaki M, Yamamoto M, Yaegashi N, et al. Identification of somatic genetic alterations in ovarian clear cell carcinoma with next generation sequencing. Genes Chromosomes Cancer. 2018;57(2):51–60.
17. Murakami R, Matsumura N, Brown JB, Higasa K, Tsutsumi T, Kamada M, Abou-Taleb H, Hosoe Y, Kitamura S, Yamaguchi K, et al. Exome Sequencing Landscape Analysis in Ovarian Clear Cell Carcinoma Shed Light on Key Chromosomal Regions and Mutation Gene Networks. Am J Pathol. 2017;187(10):2246–58.
18. Yang Q, Zhang C, Ren Y, Yi H, Luo T, Xing F, Bai X, Cui L, Zhu L, Ouyang J, et al. Genomic characterization of Chinese ovarian clear cell carcinoma identifies driver genes by whole exome sequencing. Neoplasia. 2020;22(9):399–430.
19. Kim SI, Lee JW, Lee M, Kim HS, Chung HH, Kim JW, Park NH, Song YS, Seo JS. Genomic landscape of ovarian clear cell carcinoma via whole exome sequencing. Gynecol Oncol. 2018;148(2):375–82.

20. Maru Y, Tanaka N, Ohira M, Itami M, Hippo Y, Nagase H. Identification of novel mutations in Japanese ovarian clear cell carcinoma patients using optimized targeted NGS for clinical diagnosis. Gynecol Oncol. 2017;144(2):377–83.
21. Berek JS, Kehoe ST, Kumar L, Friedlander M. Cancer of the ovary, fallopian tube, and peritoneum. Int J Gynaecol Obstet. 2018;143(Suppl 2):59–78.
22. Bolton KL, Chen D. Corona de la Fuente R, Fu Z, Murali R, Kobel M, Tazi Y, Cunningham JM, Chan ICC, Wiley BJ *et al*: Molecular Subclasses of Clear Cell Ovarian Carcinoma and Their Impact on Disease Behavior and Outcomes. Clin Cancer Res. 2022;28(22):4947–56.
23. Bolger AM, Lohse M, Usadel B. Trimmomatic: a flexible trimmer for Illumina sequence data. Bioinformatics. 2014;30(15):2114–20.
24. Li H, Durbin R. Fast and accurate short read alignment with Burrows-Wheeler transform. Bioinformatics. 2009;25(14):1754–60.
25. Okonechnikov K, Conesa A, Garcia-Alcalde F. Qualimap 2: advanced multi-sample quality control for high-throughput sequencing data. Bioinformatics. 2016;32(2):292–4.
26. Kim S, Scheffler K, Halpern AL, Bekritsky MA, Noh E, Kallberg M, Chen X, Kim Y, Beyter D, Krusche P, et al. Strelka2: fast and accurate calling of germline and somatic variants. Nat Methods. 2018;15(8):591–4.
27. Cibulskis K, Lawrence MS, Carter SL, Sivachenko A, Jaffe D, Sougnez C, Gabriel S, Meyerson M, Lander ES, Getz G. Sensitive detection of somatic point mutations in impure and heterogeneous cancer samples. Nat Biotechnol. 2013;31(3):213–9.
28. Koboldt DC, Zhang Q, Larson DE, Shen D, McLellan MD, Lin L, Miller CA, Mardis ER, Ding L, Wilson RK. VarScan 2: somatic mutation and copy number alteration discovery in cancer by exome sequencing. Genome Res. 2012;22(3):568–76.
29. Chang X, Wang K. wANNOVAR: annotating genetic variants for personal genomes via the web. J Med Genet. 2012;49(7):433–6.
30. Sondka Z, Bamford S, Cole CG, Ward SA, Dunham I, Forbes SA. The COSMIC Cancer Gene Census: describing genetic dysfunction across all human cancers. Nat Rev Cancer. 2018;18(11):696–705.
31. Li MM, Datto M, Duncavage EJ, Kulkarni S, Lindeman NI, Roy S, Tsimberidou AM, Vnencak-Jones CL, Wolff DJ, Younes A, et al. Standards and Guidelines for the Interpretation and Reporting of Sequence Variants in Cancer: A Joint Consensus Recommendation of the Association for Molecular Pathology, American Society of Clinical Oncology, and College of American Pathologists. J Mol Diagn. 2017;19(1):4–23.
32. Garrison E, Marth G: Haplotype-based variant detection from short-read sequencing. arXiv preprint arXiv:12073907 2012.
33. Hodan R, Kingham K, Cotter K, Folkins AK, Kurian AW, Ford JM, Longacre T. Prevalence of Lynch syndrome in women with mismatch repair-deficient ovarian cancer. Cancer Med. 2021;10(3):1012–7.
34. Eoh KJ, Kim JE, Park HS, Lee ST, Park JS, Han JW, Lee JY, Kim S, Kim SW, Kim JH, et al. Detection of Germline Mutations in Patients with Epithelial Ovarian Cancer Using Multi-gene Panels: Beyond BRCA1/2. Cancer Res Treat. 2018;50(3):917–25.
35. Landrum MJ, Lee JM, Benson M, Brown GR, Chao C, Chitipiralla S, Gu B, Hart J, Hoffman D, Jang W, et al. ClinVar: improving access to variant interpretations and supporting evidence. Nucleic Acids Res. 2018;46(D1):D1062–7.
36. Ng AWT, Poon SL, Huang MN, Lim JQ, Boot A, Yu W, Suzuki Y, Thangaraju S, Ng CCY. Tan P *et al*: Aristolochic acids and their derivatives are widely implicated in liver cancers in Taiwan and throughout Asia. Sci Transl Med. 2017;9(412):eaan6446.
37. Alexandrov LB, Kim J, Haradhvala NJ, Huang MN, Tian Ng AW, Wu Y, Boot A, Covington KR, Gordenin DA, Bergstrom EN, et al. The repertoire of mutational signatures in human cancer. Nature. 2020;578(7793):94–101.
38. Favero F, Joshi T, Marquard AM, Birkbak NJ, Krzystanek M, Li Q, Szallasi Z, Eklund AC. Sequenza: allele-specific copy number and mutation profiles from tumor sequencing data. Ann Oncol. 2015;26(1):64–70.
39. Dewhurst SM, McGranahan N, Burrell RA, Rowan AJ, Gronroos E, Endesfelder D, Joshi T, Mouradov D, Gibbs P, Ward RL, et al. Tolerance of whole-genome doubling propagates chromosomal instability and accelerates cancer genome evolution. Cancer Discov. 2014;4(2):175–85.
40. Wilkerson MD, Hayes DN. ConsensusClusterPlus: a class discovery tool with confidence assessments and item tracking. Bioinformatics. 2010;26(12):1572–3.
41. Gerstung M, Jolly C, Leshchiner I, Dentro SC, Gonzalez S, Rosebrock D, Mitchell TJ, Rubanova Y, Anur P, Yu K, et al. The evolutionary history of 2,658 cancers. Nature. 2020;578(7793):122–8.
42. Shih Ie M, Panuganti PK, Kuo KT, Mao TL, Kuhn E, Jones S, Velculescu VE, Kurman RJ, Wang TL. Somatic mutations of PPP2R1A in ovarian and uterine carcinomas. Am J Pathol. 2011;178(4):1442–7.
43. Nguyen L. J WMM, Van Hoeck A, Cuppen E: Pan-cancer landscape of homologous recombination deficiency. Nat Commun. 2020;11(1):5584.
44. Wu RC, Ayhan A, Maeda D, Kim KR, Clarke BA, Shaw P, Chui MH, Rosen B, Shih Ie M, Wang TL. Frequent somatic mutations of the telomerase reverse transcriptase promoter in ovarian clear cell carcinoma but not in other major types of gynaecological malignancy. J Pathol. 2014;232(4):473–81.
45. Huang DS, Wang Z, He XJ, Diplas BH, Yang R, Killela PJ, Meng Q, Ye ZY, Wang W, Jiang XT, et al. Recurrent TERT promoter mutations identified in a large-scale study of multiple tumour types are associated with increased TERT expression and telomerase activation. Eur J Cancer. 2015;51(8):969–76.
46. Watkins TBK, Lim EL, Petkovic M, Elizalde S, Birkbak NJ, Wilson GA, Moore DA, Gronroos E, Rowan A, Dewhurst SM, et al. Pervasive chromosomal instability and karyotype order in tumour evolution. Nature. 2020;587(7832):126–32.
47. McGranahan N, Favero F, de Bruin EC, Birkbak NJ, Szallasi Z, Swanton C. Clonal status of actionable driver events and the timing of mutational processes in cancer evolution. Sci Transl Med. 2015;7(283):283ra254.
48. Pujade-Lauraine E, Ledermann JA, Selle F, Gebski V, Penson RT, Oza AM, Korach J, Huzarski T, Poveda A, Pignata S, et al. Olaparib tablets as maintenance therapy in patients with platinum-sensitive, relapsed ovarian cancer and a BRCA1/2 mutation (SOLO2/ENGOT-Ov21): a double-blind, randomised, placebo-controlled, phase 3 trial. Lancet Oncol. 2017;18(9):1274–84.
49. Kristeleit R, Lisyanskaya A, Fedenko A, Dvorkin M, de Melo AC, Shparyk Y, Rakhmatullina I, Bondarenko I, Colombo N, Svintsitskiy V, et al. Rucaparib versus standard-of-care chemotherapy in patients with relapsed ovarian cancer and a deleterious BRCA1 or BRCA2 mutation (ARIEL4): an international, open-label, randomised, phase 3 trial. Lancet Oncol. 2022;23(4):465–78.
50. Marabelle A, Le DT, Ascierto PA, Di Giacomo AM, De Jesus-Acosta A, Delord JP, Geva R, Gottfried M, Penel N, Hansen AR, et al. Efficacy of Pembrolizumab in Patients With Noncolorectal High Microsatellite Instability/Mismatch Repair-Deficient Cancer: Results From the Phase II KEYNOTE-158 Study. J Clin Oncol. 2020;38(1):1–10.
51. Rugo HS, Lerebours F, Ciruelos E, Drullinsky P, Ruiz-Borrego M, Neven P, Park YH, Prat A, Bachelot T, Juric D, et al. Alpelisib plus fulvestrant in PIK3CA-mutated, hormone receptor-positive advanced breast cancer after a CDK4/6 inhibitor (BYLieve): one cohort of a phase 2, multicentre, open-label, non-comparative study. Lancet Oncol. 2021;22(4):489–98.
52. Konstantinopoulos PA, Barry WT, Birrer M, Westin SN, Cadoo KA, Shapiro GI, Mayer EL, O'Cearbhaill RE, Coleman RL, Kochupurakkal B, et al. Olaparib and alpha-specific PI3K inhibitor alpelisib for patients with epithelial ovarian cancer: a dose-escalation and dose-expansion phase 1b trial. Lancet Oncol. 2019;20(4):570–80.
53. Wiedemeyer K, Wang L, Kang EY, Liu S, Ou Y, Kelemen LE, Feil L, Anglesio MS, Glaze S, Ghatage P, et al. Prognostic and Theranostic Biomarkers in Ovarian Clear Cell Carcinoma. Int J Gynecol Pathol. 2022;41(2):168–79.
54. Janne PA, Riely GJ, Gadgeel SM, Heist RS, Ou SI, Pacheco JM, Johnson ML, Sabari JK, Leventakos K, Yau E, et al. Adagrasib in Non-Small-Cell Lung Cancer Harboring a KRAS(G12C) Mutation. N Engl J Med. 2022;387(2):120–31.
55. Skoulidis F, Li BT, Dy GK, Price TJ, Falchook GS, Wolf J, Italiano A, Schuler M, Borghaei H. Barlesi F *et al*: Sotorasib for Lung Cancers with KRAS p.G12C Mutation. N Engl J Med. 2021;384(25):2371–81.
56. Mao Z, Xiao H, Shen P, Yang Y, Xue J, Yang Y, Shang Y, Zhang L, Li X, Zhang Y, et al. KRAS(G12D) can be targeted by potent inhibitors via formation of salt bridge. Cell Discov. 2022;8(1):5.
57. Knudson AG. Hereditary cancer: two hits revisited. J Cancer Res Clin Oncol. 1996;122(3):135–40.
58. Alldredge JK, Eskander RN. EZH2 inhibition in ARID1A mutated clear cell and endometrioid ovarian and endometrioid endometrial cancers. Gynecol Oncol Res Pract. 2017;4:17.

59. O'Connor CM, Taylor SE, Miller KM, Hurst L, Haanen TJ, Suhan TK, Zawacki KP, Noto FK, Trako J, Mohan A, et al. Targeting Ribonucleotide Reductase Induces Synthetic Lethality in PP2A-Deficient Uterine Serous Carcinoma. Cancer Res. 2022;82(4):721–33.
60. Yuan X, Larsson C, Xu D. Mechanisms underlying the activation of TERT transcription and telomerase activity in human cancer: old actors and new players. Oncogene. 2019;38(34):6172–83.
61. Weng CH, Wu RC, Chen SJ, Chen HC, Tan KT, Lee YS, Huang SS, Yang LY, Wang CJ, Chou HH, et al. Molecular evidence for a clonal relationship between synchronous uterine endometrioid carcinoma and ovarian clear cell carcinoma: a new example of "precursor escape"? J Mol Med (Berl). 2021;99(7):959–66.
62. Suda K, Nakaoka H, Yoshihara K, Ishiguro T, Tamura R, Mori Y, Yamawaki K, Adachi S, Takahashi T, Kase H, et al. Clonal Expansion and Diversification of Cancer-Associated Mutations in Endometriosis and Normal Endometrium. Cell Rep. 2018;24(7):1777–89.
63. Horikawa I, Cable PL, Mazur SJ, Appella E, Afshari CA, Barrett JC. Downstream E-box-mediated regulation of the human telomerase reverse transcriptase (hTERT) gene transcription: evidence for an endogenous mechanism of transcriptional repression. Mol Biol Cell. 2002;13(8):2585–97.
64. Schnack TH, Oliveira DNP, Christiansen AP, Hogdall C, Hogdall E. Prognostic impact of molecular profiles and molecular signatures in clear cell ovarian cancer. Cancer Genet. 2023;278–279:9–16.
65. Katagiri A, Nakayama K, Rahman MT, Rahman M, Katagiri H, Nakayama N, Ishikawa M, Ishibashi T, Iida K, Kobayashi H, et al. Loss of ARID1A expression is related to shorter progression-free survival and chemoresistance in ovarian clear cell carcinoma. Mod Pathol. 2012;25(2):282–8.
66. Steele CD, Abbasi A, Islam SMA, Bowes AL, Khandekar A, Haase K, Hames-Fathi S, Ajayi D, Verfaillie A, Dhami P, et al. Signatures of copy number alterations in human cancer. Nature. 2022;606(7916):984–91.

Publisher's Note